Sensors & Transducers, Vol. 170, Issue 5, May 2014, pp. 234-240

Sensors & Transducers

http://www.sensorsportal.com

Phase Information for Classification Between Clench Speed and Clench Force Motor Imagery

[1, 2] Baolei XU, [3] Yunfa FU, [1] Gang SHI, [1, 2] Xuxian YIN, [1, 4] Zhidong WANG and [1, 5] Hongyi LI

[1] State Key Laboratory of Robotics, Shenyang Institute of Automation (SIA), Chinese Academy of Sciences (CAS), Shenyang 110016, P. R. China
[2] University of Chinese Academy of Sciences, Beijing 100049, P. R. China
[3] School of Automation and Information Engineering, Kunming University of Science and Technology, Kunming 650500, P. R. China
[4] Dept. of Advanced Robotics, Chiba Institute of Technology, Chiba 2750016, Japan
[5] School of Mechanical Engineering & Automation, Northeastern University, Shenyang, China
[1] Tel.: +86-24-23970721, fax: +86-24-23970021
E-mail: blxu@sia.cn

Received: 28 February 2014 /Accepted: 30 April 2014 /Published: 31 May 2014

Abstract: In this paper, we investigate the phase information for classification between clench speed and clench force motor imagery for BCI applications. The multivariate extensions of empirical mode decomposition (MEMD) are used to decompose EEG data into intrinsic mode functions (IMFs). Then, the phase information is got by transforming IMFs into analytic signal using Hiblert transforms. Six feature types are compared in the paper for channel C3, Cz and C4: the amplitude of IMFs, the power of IMFs, the amplitude of the corresponding analytic signal, the instantaneous phase of the analytic signal, the instantaneous frequency of the analytic signal and the phase-locking value (PLV) between two channels. The support vector machine with 5-fold cross-validation is used to classify clench speed motor imagery from clench force motor imagery. The results show that for some subjects the instantaneous phase can get the best results, while PLV never performs best compared with other features. The minimum classification error rate of 0.25 is reached in our research. *Copyright © 2014 IFSA Publishing, S. L.*

Keywords: Phase, Brain-computer interface (BCI), MEMD, Hilbert transform, motor parameters imagery.

1. Introduction

Brain-computer interface (BCI) is an emerging technology to realize environment and device control using brain signals directly. The concept of BCI was coined by Vidal in 1970s [1]. Due to the restrictions in hardware and software capacities, this technology developed very slowly before 1990s. However, with the rapid development in micro-electronics and artificial intelligent (AI), the technology has got many important achievements in recent 20 years. Currently, researchers around the world are applying BCI to the field of neurological rehabilitation [2], prosthetic control [3], cursor control [4], wheelchair control [5] and computer games [6]. More than that, BCI has taken the first step from the laboratory to the market, such as the Mind-Wave from NeuroSky Inc. and the XWave from PLX Devices Inc.

A BCI system consists of three parts [7]: the neural sensor that acquires the intent related neural activity signals; the decoder that translates the physiological signals into control commands, and the actuator that execute the commands to complete the user intend.

The physiological signals that can be detected by neural sensors can be divided into three categories. The first one is the bio-electrical signals [8], including the non-invasive electroencephalography (EEG), the semi-invasive electrocardiography (ECoG), and the fully invasive microelectrode-based intracortical spikes and local field potentials (LFPs). The second one is the bio-magnetic signals, and currently the non-invasive magnetocencephalography (MEG) is only one kind of such signal used in BCI. The last one is the hemodynamic signals, such as the functional magnetic resonance imaging (fMRI) signals and the near-infrared spectroscopy (NIRS) signals. fMRI measures BOLD (blood oxygen level dependent) hemodynamic response, and NIRS measures the oxygenated and deoxygenated hemoglobin changes. Both the two methods are non-invasive and are highly correlated [9]. Among all the signal types, EEG and NIRS are used mostly in the world because their low cost and portability, especially EEG.

Many researches show that the motor imagery shares the same neural substrate with the executed movements [10], so motor imagery can be used to modulate EEG signals to provide features for the decoder and then realize devices control through the actuator. It is widely accepted that motor imagery can generate a power decrease and/or a power enhancement of specified frequency bands (event-related de-synchronization, ERD, and event-related synchronization, ERS), and ERD/ERS is the mostly used feature for motor imagery based BCI systems [11]. Common Spatial Patterns (CSP) outlined by Müller-Gerking is another widely used method to discriminate motor imagery types [12], and many variations of CSP have been proposed in recent years, such as Sub-band Common Spatial Pattern (SBCSP) [13] and Filter Bank Common Spatial Pattern (FBCSP) [14]. However, CSP requires a large number of channels to get a good result, thus the subject needs more time to prepare before the usage of a BCI system [15].

Phase also plays an important role when different brain regions communicate with each other to complete cognitive tasks [16]. The first measure of phase covariance between two EEG signals was proposed by Lachaux et al. as the phase-locking value (PLV) [17]. Compared with the coherence method, the advantage of PLV is its capacity to separate amplitude and phase information. Gysels et al. compared the PLV with spectral coherence and spectral density, and they noticed significant differences between the three different feature types [18]. Then, they further investigated the broadband and narrowband phase features using FIR bandpass filters, and their results showed that while narrow band power features generated better results than broad band features, broad band PLV features generated better results than narrow band ones [19]. However, in both literatures, the authors using different methods to preprocess the phase features and band power features, which may lead to their results less credible. Sweeney-reed et al. first introduced the empirical mode decomposition (EMD) method to the phase synchronization detection for processing the neural assemblies, and their results implied that the EMD method can improve the time-frequency localization of phase synchrony than the band pass filtering method [20]. Another advantage of EMD is that it can avoid arbitrary cut-off selection for band-pass filter, which may markedly influence synchrony detection [21]. Then, Looney et al. introduced complex extensions of EMD to assure the same decomposition levels for analysis of channel pairs [22]. Furthermore, the recently developed multivariate extensions of empirical mode decomposition (MEMD) are used to get frequency information in motor imagery BCI [23].

In this paper, we apply MEMD to analyze the phase information underling motor parameters imagination. Subjects are instructed to do clench speed and clench force motor imagery in the experiment. Compared with other BCI paradigms that instruct subjects to imagine movements of different body parts, such as left hand, right hand, foot, and tongue [24], our paradigm can increase BCI's control commands, thus improves the feasibility for application of devices control [25, 26].

The paper is constructed as follows. Section 2 describes the experiment design in our research. Then, we introduce the procedure to get phase information and the classification method to distinguish different motor imagery tasks in section 3. Subsequently, the classification results are presented in section 4. Finally, in section 5, we discuss the results in our research and make some conclusions.

2. Subjects and Experiment Paradigm

2.1. Subjects

Six healthy subjects participate in the experiment (three male, three female), and their average age is 26.8 years. All of them are right-handed, and they all give written approval to take part in the research. To research the training effect on classification accuracy, they are divided into two groups. One group is trained three times before the experiment, while the other group is not trained, and they are simply instructed how to complete the tasks during the experiment. The experiment is approved by the Ethical Committee of the Shenyang Institute of Automation (SIA), Chinese Academy of Sciences (CAS).

2.2. Experiment Paradigm

In our experiment, subjects are instructed to do right hand clench speed motor imagery and right hand clench force motor imagery, as motor parameters imagery can increase BCI's control number, and thus improve the flexibility for applications such as wheelchair control, prosthesis control, and environment control.

Subjects execute clench speed exercise at frequencies of 0.5 Hz, 1 Hz, and 2 Hz ac-cording to a metronome. The executed clench force exercise is done with the help of a grip dynamometer. The maximum clench force (MF) of each subject is measured, and they are instructed to clench the grip dynamometer to 20 % MF, 50 % MF and 80 % MF in one second, and then hold it during the left four seconds. The entire subject is instructed to remember the feeling when they do the exercises, and recall the feeling during the task period in the experiment. The reason to refine clench speed motor imagery and clench force imagery is to balance the motor parameter difference for every subject, and thus the results in the paper are more reliable.

A single trial is divided into four parts, as shown in Fig. 1. Ten seconds base-line time followed by two seconds cue time to inform the subject which motor imagery task to execute in the next ten seconds task period. After that is the rest period that lasts ten to twelve seconds. In our experiment, the time for a single trial is much longer than other EEG based paradigms because we acquire the functional near-infrared spectroscopy (fNIRS) signal simultaneously with the EEG signal. However, we only investigate the EEG signal in this paper, and the EEG-fNIRS combined signal will be studied in the near future.

Every subject take part in three sessions, and each session contains sixty trials. The trial number of every motor imagery type equals to each other.

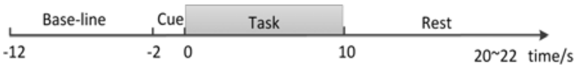

Fig. 1. The event procedure during a trial. In our experiment, the time duration of a trial is much longer than other EEG based experiments. The reason for this is that we acquire functional near-infrared spectroscopy (fNIRS) signals simultaneously with EEG signals. Due to the nature of hemodynamic responses, fNIRS signals take much longer time to return to the base line than EEG signals.

2.3. Data Acquisition

We use the Neuroscan synamps2 to acquire EEG signals at a sampling frequency of 1000 Hz. Twenty-one Ag/AgCl electrodes over parietal area are used: FC5, FC3, FC1, FCz, FC2, FC4, FC6, C5, C3, C1, Cz, C2, C4, C6, CP5, CP3, CP1, CPz, CP2, CP4, and CP6. A1 is used as the reference electrode, and FPz is used as the ground electrode. All the electrode impedance is lower than 5 kOhm. An online notch filter is used to eliminate the 50 Hz power line noise.

3. Signal Processing Methods

3.1. Preprocessing Methods

To alleviate the computational cost, the EEG data are down-sampled to 100 Hz. Before the down-sample process, the data are low passed using an IIR filter at a cutoff frequency of 50 Hz to avoid the distortion due to down-sampling. Then, to remove the low frequency drift, a band-pass filter at the cutoff frequency of 0.5 Hz and 45 Hz is used to filter the data. Both the low-pass filter used for down-sampling and the band-pass filter are applied in both the forward and backward directions to achieve zero-phase distortion. After that, a small Laplacian filter is used to improve the spatial resolution of all the EEG channels [27].

3.2. Multivariate Empirical Mode Decomposition (MEMD)

Empirical mode decomposition (EMD) was developed by Huang et al. for nonlinear and non-stationary signal analysis [28]. This method decompose data set into a number of 'intrinsic mode functions' (IMFs) through iteration approach, and the resulting IMFs can be processed using Hilbert transforms to get instantaneous frequencies. The decomposition process is adaptive and very efficient without any prior knowledge needed. However, EMD is only suitable for one channel data, because when two or more channels are decomposed using EMD independently, the resulting IMFs at the same level corresponding to different channels usually have different frequency range. To address this disadvantage, the bivariate empirical mode decomposition (BEMD) is proposed to solve the two channel problem in 2007 [29], and then the multivariate empirical mode decomposition (MEMD) are proposed in 2010 to solve the problem of more than 3 channels [30]. In this paper, the MEMD is used to decompose EEG data from C3, Cz, and C4 simultaneously, and the IMFs get from the three channels are shown in Fig. 2. It is obviously that the IMFs at the same level from the three channels have the same frequency range, which is necessary for the following feature extraction process.

3.3. Hilbert Transforms

After we get the IMFs of EEG data, we can get the phase information of IMFs by two methods. The first one is to convert the signal to its analytic format by Hilbert transform, and the other one is to convolute the signal with a complex wavelet [17].

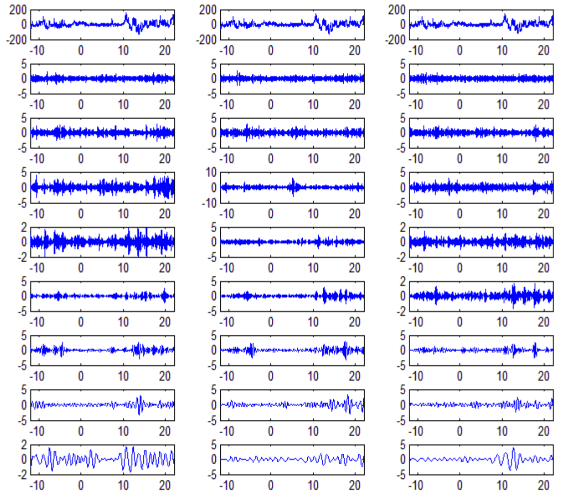

Fig. 2. The EEG signal and the corresponding IMFs for channel C3, Cz and C4. The left column is from channel C3, the middle column is from channel Cz, and the right column is from channel C4. The top row is the original EEG data, and the following 8 rows are the corresponding IMFs of level 1 to 8.

Both the two methods can get comparable results [31].

In this paper, we choose the Hilbert transform method. For a signal *x(t)*, its Hilbert transform is thought as the convolution with the function

$$\begin{aligned} h(t) &= \frac{1}{\pi t} \\ y(t) &= P\int_{-\infty}^{\infty} x(\tau)h(t-\tau)d\tau = \frac{1}{\pi}P\int_{-\infty}^{\infty}\frac{x(\tau)}{t-\tau}d\tau, \end{aligned} \qquad (1)$$

where P is the Cauchy principal value. Then, we can get the analytic signal of *x(t)*,

$$z(t) = x(t) + iy(t) = A(t)e^{i\theta(t)}, \qquad (2)$$

where i is the imaginary unit, $A(t)=sqrt\ (x(t)^2+y(t)^2$ is the instantaneous amplitude, and $\theta(t)=arctan\ y(t)/x(t)$ is the instantaneous phase. The angle range of $\theta(t)$ is [-π π], and to get instantaneous frequency using $w(t)=d\theta(t)/d(t)$, $\theta(t)$ must be unwrapped by adding multiples of ±2 π when absolute jumps of more than π happens between consecutive elements.

3.4. Feature Extraction

In this paper, we apply MEMD to three channels C3, Cz and C4 to reduce the computation cost, and the resulting IMFs with mean frequency more than 4 Hz are chosen in the following feature extraction process. Five feature types are compared for single channel IMFs: the amplitude of IMFs ('imf'), the power of IMFs ('power'), the amplitude of the corresponding analytic signal ('Amp'), the instantaneous phase of the analytic signal ('Angle'), and the instantaneous frequency of the analytic signal ('Frequency'). The difference of these five feature types are used for two channel combinations (C3-Cz, C4-Cz and C3-C4), as well as PLV [17],

$$\mathrm{PLV}_t = \frac{1}{N}\left|\sum_{n=1}^{N}\exp(j(\theta_1(t,n)-\theta_2(t,n)))\right|, \qquad (3)$$

PLV measures the phase variability between two channels. Its range is [0 1], where 0 means no synchrony between two channels, and 1 means total synchrony between two channels. In our research, the N is set as the sampling frequency.

All the features are averaged using a 1 second time windows with step of 0.125 s, which is a reasonable configuration for online BCI applications.

E. Support vector machines

The different IMFs features are used to classify clench speed motor imagery from clench force motor imagery using support vector machines (SVM) [32]. Compared with other machine learning methods, SVM can get the best classification plane between two classes, and address the linear un-separable problem using kernel functions. In our research, we choose the linear kernel $K(x_i, x_j) = x_i^T x_j$, as this kernel has minimum parameters to optimize.

Features of four time range are tried in the paper: [-1 1], [-1 0], [0 1] and [-0.5 0.5]. Our results show that the range [-0.5 0.5] can get the minimum classification error rate. The 5-fold cross-validation is used to make our results more reliable.

4. Results

The minimum classification error rate using the best feature type is shown in Table 1, and the corresponding channel type, feature type and frequency range of IMFs are shown in Table 2. For the entire subject, a mean error rate of 0.30 can be got. The mean minimum error rate for three trained subjects is 0.27, and the mean minimum error rate for three untrained subjects is 0.32. These results mean that the training process is essential to get better classification results.

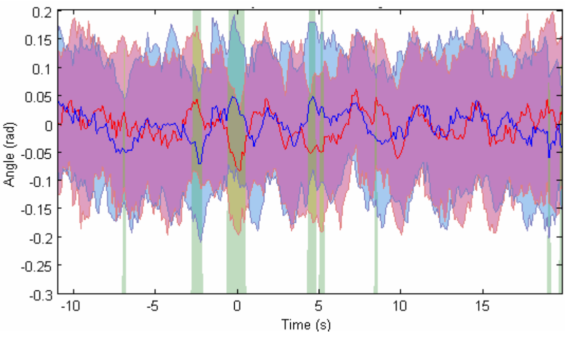

Fig. 3. The instantaneous phase difference between channel C3 and Cz for one subject.

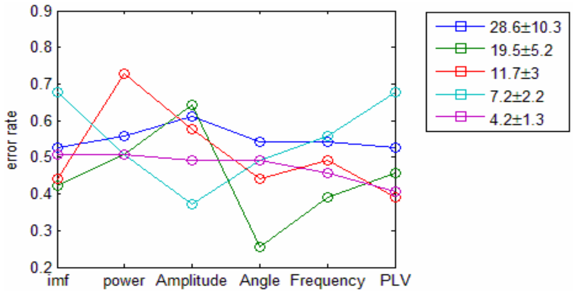

Fig. 4. The resulting error rate using different IMFs and feature types.

Table 1. The minimum error rate using the best feature type.

	Session 1	Session 2	Session 3	Mean
Subject 1	0.32	0.25	0.27	0.28
Subject 2	0.27	0.25	0.25	0.26
Subject 3	0.28	0.39	0.32	0.33
Subject 4	0.35	0.28	0.33	0.32
Subject 5	0.28	0.35	0.27	0.30
Subject 6	0.30	0.28	0.27	0.28

Due to the variability of EEG signals, the best feature types change for every session. For some subjects, the feature of IMFs power can get the minimum results; for some paper, the feature of instantaneous phase can get the minimum results, as is shown in Fig. 3 and Fig. 4.

Even for the same subject, the best feature types change between different sessions. This is reasonable, and this is why calibration is needed before a subject uses a BCI system. Our results also show that PLV feature cannot get the minimum error rate, which is consistent with Li's results [33].

Table 2. The channel name, feature type and frequency range corresponding to the results in Table 1.

	Session 1			Session 2			Session 3		
	Channel	**Feature**	**Frequency (Hz)**	**Channel**	**Feature**	**Frequency (Hz)**	**Channel**	**Feature**	**Frequency (Hz)**
1	C3	Angle	15.4+-5.2	C3-Cz	power	12.1+-3.4	C4-Cz	Amp	6.8+-2
2	C3-C4	Freq	7.3+-2.3	C3-Cz	Angle	19.5+-5.2	Cz	imf	8.5+-2.5
3	C3-Cz	imf	19.5+-5.8	C3-Cz	power	4.2+-7.9	Cz	power	6.9+-2.2
4	C4	power	10+-10.4	C4-Cz	Freq	6.3+-1.9	C4-Cz	imf	28.8+-11.2
5	C3-C4	Angle	10.3+-10.3	C4	Amp	20.5+-5.	C3-Cz	power	19.2+-5.3
6	Cz	power	29.2+-14	Cz	Amp	31.8+-12.1	C3-Cz	Amp	18.9+-5.9

5. Discussions and Conclusions

In this paper, the instantaneous phase information is investigated using MEMD decomposition and Hilbert transforms for clench speed and clench force motor imagery. We compared six feature types: the amplitude of IMFs, the power of IMFs, the amplitude of analytic signals, the instantaneous phase of analytic signals, the instantaneous frequency of IMFs and the PLV between two channels. The results show that the best feature type changes between subjects and sessions. This is reasonable because of the high variability of EEG signals.

The mean minimum classification error rate between clench speed and clench force motor imagery is 0.30, which means that the motor parameter imagery paradigm can be used in BCI systems and may provide more precise control commands for devices such as wheelchair and prosthesis. The mean minimum error rate for three trained subjects is 0.27, and the mean minimum error rate for three un-trained subjects is 0.32, which means that sufficient training is essential for a BCI user to get better control results.

While most of BCI researchers pay attention to time-spatial-frequency features to improve classification results, our results show that the instantaneous phase can get better results for some subjects in some sessions. Our research also shows that the instantaneous phase is more suitable for BCI applications, which is consistent with Li's research [33].

In our future research, we will combine the EEG and NIRS signal together, and investigate whether the classification results can be improved by optimum feature combinations.

Acknowledgement

This work is supported by the National High Technology Research and Development Program of China (863 Program) under Grant No. 2012AA02A605, and National Natural Science Foundation (NNSF) of China under Grant No. 61203368 and 61102014.

References

[1]. J. Vidal, Toward direct brain-computer communication, *Annual Review of Biophysics & Bioengineering*, Vol. 2, 1973, pp. 157-80.

[2]. G. R. Muller-Putz, C. Pokorny, D. S. Klobassa, and P. Horki, A single-switch BCI based on passive and imagined movements: toward restoring communication in minimally conscious patients, *International Journal of Neural Systems*, Vol. 23, Issue 2, 2013, 1250037.

[3]. G. A. Tabot, J. F. Dammann, J. A. Berg, F. V. Tenore, J. L. Boback, R. J. Vogelstein, and S. J. Bensmaia, Restoring the sense of touch with a prosthetic hand through a brain interface, *Proceedings of the National Academy of Sciences of the United States of America*, Vol. 110, Issue 45, 2013, pp. 18279-18284.

[4]. J. Long, Y. Li, T. Yu, and Z. Gu, Target Selection With Hybrid Feature for BCI-Based 2-D Cursor Control, *IEEE Transactions on Biomedical Engineering*, Vol. 59, Issue 1, 2012, pp. 132-140.

[5]. Y. Q. Li, J. H. Pan, F. Wang, and Z. L. Yu, A Hybrid BCI System Combining P300 and SSVEP and Its Application to Wheelchair Control, *IEEE Transactions on Biomedical Engineering*, Vol. 60, Issue 11, 2013, pp. 3156-3166.

[6]. B. van de Laar, H. Gurkok, D. P. O. Bos, M. Poel, and A. Nijholt, Experiencing BCI Control in a Popular Computer Game, *IEEE Transactions on Computational Intelligence and Ai in Games*, Vol. 5, Issue 2, 2013, pp. 176-184.

[7]. L. R. Hochberg, and J. P. Donoghue, Sensors for brain-computer interfaces, *IEEE Engineering in Medicine and Biology Magazine,* Vol. 25, Issue 5, 2006, pp. 32-38.

[8]. J. J. Daly, and J. R. Wolpaw, Brain-computer interfaces in neurological rehabilitation, *Lancet Neurology*, Vol. 7, Issue 11, 2008, pp. 1032-1043.

[9] X. Cui, S. Bray, D. M. Bryant, G. H. Glover, and A. L. Reiss, A quantitative comparison of NIRS and fMRI across multiple cognitive tasks, *Neuroimage*, Vol. 54, Issue 4, 2011, pp. 2808-2821.

[10]. M. L. Stavrinou, L. Moraru, L. Cimponeriu, S. Della Penna, and A. Bezerianos, Evaluation of cortical connectivity during real and imagined rhythmic finger tapping, *Brain Topography*, Vol. 19, Issue 3, 2007. pp. 137-145.

[11]. G. Pfurtscheller, and F. H. Lopes da Silva, Event-related EEG/MEG synchronization and desynchronization: basic principles, *Clinical Neurophysiology*, Vol. 110, Issue 11, 1999, pp. 1842-57.

[12]. J. Müller-Gerking, G. Pfurtscheller, and H. Flyvbjerg, Designing optimal spatial filters for single-trial EEG classification in a movement task, *Clinical Neurophysiology*, Vol. 110, Issue 5, 1999, pp. 787-798.

[13]. Q. Novi, G. Cuntai, T. H. Dat, and X. Ping, Sub-band Common Spatial Pattern (SBCSP) for Brain-Computer Interface, in *Proceedings of the Conference on Neural Engineering IEEE/EMBS*. 2007, pp. 204-207.

[14]. K. K. Ang, Z. Y. Chin, H. Zhang, C. Guan, and IEEE, Filter Bank Common Spatial Pattern (FBCSP) in Brain-Computer Interface, in *Proceedings of the IEEE International Joint Conference on Neural Networks*, 2008. pp. 2390-2397.

[15]. G. Townsend, B. Graimann, and G. Pfurtscheller, A comparison of common spatial patterns with complex band power features in a four-class BCI experiment, *IEEE Transactions on Biomedical Engineering*, Vol. 53, Issue 4, 2006, pp. 642-651.

[16]. E. Rodriguez, N. George, J.-P. Lachaux, J. Martinerie, B. Renault, and F. J. Varela, Perception's shadow: long-distance synchronization of human brain activity, *Nature*, Vol. 397, Issue 6718, 1999, pp. 430-433.

[17]. J.-P. Lachaux, E. Rodriguez, J. Martinerie, and F. J. Varela, Measuring phase synchrony in brain signals, *Human Brain Mapping*, Vol. 8, Issue 4, 1999, pp. 194-208.

[18]. E. Gysels, and P. Celka, Phase synchronization for the recognition of mental tasks in a brain-computer interface, *IEEE Transactions on Neural Systems and Rehabilitation Engineering*, Vol. 12, Issue 4, 2004, pp. 406-415.

[19]. E. Gysels, P. Renevey, and P. Celka, SVM-based recursive feature elimination to compare phase synchronization computed from broadband and narrowband EEG signals in Brain-Computer Interfaces, *Signal Processing*, Vol. 85, Issue 11, 2005, pp. 2178-2189.

[20]. C. M. Sweeney-reed, and S. J. Nasuto, A novel approach to the detection of synchronisation in EEG based on empirical mode decomposition, *Journal of Computational Neuroscience*, Vol. 23, Issue 1, 2007, pp. 79-111.

[21]. C. M. Sweeney-Reed, and S. J. Nasuto, Detection of neural correlates of self-paced motor activity using empirical mode decomposition phase locking analysis, *Journal of Neuroscience Methods*, Vol. 184, Issue 1, 2009, pp. 54-70.

[22]. D. Looney, C. Park, P. Kidmose, M. Ungstrup, and D. P. Mandic, Measuring phase synchrony using complex extensions of EMD, in *Proceedings of the 15th IEEE Workshop on Statistical Signal Processing*, 2009, pp.49-52.

[23]. C. Park, D. Looney, N. U. Rehman, A. Ahrabian, and D. P. Mandic, Classification of Motor Imagery BCI Using Multivariate Empirical Mode Decomposition. *IEEE Transactions on Neural Systems and Rehabilitation Engineering*, Vol. 21, Issue 1, 2013, pp. 10-22.

[24]. Sano, A. and H. Bakardjian, Movement-Related Cortical Evoked Potentials Using Four-Limb Imagery, *International Journal of Neuroscience*, Vol. 119, Issue 5, 2009, pp. 639-663.

[25]. N. Robinson, A. P. Vinod, K. K. Ang, K. P. Tee, and C. T. T. Guan, EEG-Based Classification of Fast and Slow Hand Movements Using Wavelet-CSP Algorithm, *IEEE Transactions on Biomedical Engineering*, Vol. 60, Issue 8, 2013, pp. 2123-2132.

[26]. M. Jochumsen, I. K. Niazi, N. Mrachacz-Kersting, D. Farina, and K. Dremstrup, Detection and classification of movement-related cortical potentials associated with task force and speed, *Journal of Neural Engineering*, Vol. 10, Issue 5, 2013, 056015.

[27]. D. J. McFarland, L. M. McCane, S. V. David, and J. R. Wolpaw, Spatial filter selection for EEG-based communication, *Electroencephalography and Clinical Neurophysiology*, Vol. 103, Issue 3, 1997, pp. 386-394.

[28]. N. E. Huang, Z. Shen, S. R. Long, M. C. Wu, H. H. Shi, and Q. Zheng, The empirical mode decomposition and the Hilbert spectrum for nonlinear and non-stationary time series analysis, *Proceedings of the Royal Society of London. Series A: Mathematical, Physical and Engineering Sciences*, Vol. 454, No. 1971, March 1998, pp. 903-995

[29]. G. Rilling, P. Flandrin, P. Gonalves, and J. M. Lilly, Bivariate Empirical Mode Decomposition, *IEEE Signal Processing Letters*, Vol. 14, Issue 12, 2007, pp. 936-939.

[30]. N. Rehman, and D. P. Mandic, Multivariate empirical mode decomposition, *Proceedings of the Royal Society A: Mathematical, Physical and Engineering Sciences*, Vol. 466, Issue 2117, 2010, pp. 1291-1302.

[31]. M. Le Van Quyen, J. Foucher, J. Lachaux, E. Rodriguez, A. Lutz, J. Martinerie, and F. J. Varela, Comparison of Hilbert transform and wavelet methods for the analysis of neuronal synchrony, *Journal of Neuroscience Methods*, Vol. 111, Issue 2, 2001, pp. 83-98.

[32]. C. Cortes and V. Vapnik, Support-Vector Networks, *Machine Learning*, Vol. 20, Issue 3, 1995, pp. 273-297.

[33]. J. I. E. Li and L. Zhang, Phase interval value analysis for the motor imagery task in bci, *Journal of Circuits, Systems and Computers*, Vol. 18, Issue 8, 2009, pp. 1441-1452.